

Scaling of Icing Tests: A Review of Recent Progress

R. J. Kind*

Carleton University, Ottawa, Ontario K1S 5B6, Canada

Recent progress in development of scaling methods for icing testing at reduced scale, with the focus on glaze icing, is reviewed. In most glaze icing tests it is now recognized that it is necessary to match test values of an accumulation parameter, of a droplet inertia parameter, and of the freezing fraction at the stagnation point to the values in the reference case. Evidence has been presented in recent years that surface tension effects are also important and must be correctly scaled to obtain valid test results. A Weber number is proposed as an additional scaling parameter for this purpose. It is based on a measure of the thickness of the liquid water flow that exists on the surface of accreting glaze ice. Assessment of the proposed Weber number, using results available in the literature and from purpose-designed tests, suggests that it has merit. Evidence is also presented showing that the distribution of freezing fraction over the ice accretion is not matched, as it should be, unless freestream air temperature is the same as in the reference case. An analysis shows that if test run conditions are determined as outlined in the paper then the Weber number based on droplet diameter will automatically be approximately equal to the reference value; this fortunate circumstance implies that splashing at droplet impingement would also be correctly scaled. A tentative conclusion is that satisfactory results appear to be obtainable from reduced-scale glaze icing tests, at least for moderate size-reduction ratios.

Nomenclature

A, B	= sensible-to-latent heat ratio and convective-to-latent heat ratio [see Eq. (2) and Appendix]
Ac	= accumulation parameter (see Appendix)
C_f	= skin-friction coefficient, $\tau_0/0.5\rho V^2$
C_w	= specific heat of liquid water
c	= chord length
d, D	= droplet median volume diameter, diameter of body nose region
h_c	= convective heat-transfer coefficient
h_{fs}	= latent heat of fusion of water
K	= droplet trajectory parameter (see Appendix)
ℓ, L	= general length scale; body length scale
m_i, m_r	= impingement and runback mass flow rate per unit area of liquid water into energy-balance control volume
n, n_0	= freezing fraction, freezing fraction at stagnation point
p	= static pressure
q_e/q_c	= ratio of evaporative to dry convective heat transfer
T_i	= temperature of ice accretion surface (273 K or 0°C for glaze icing)
T_∞, T_R	= static temperature and recovery temperature of freestream air
t_w	= thickness of liquid water film; Eq. (1)
u_w	= mean velocity in liquid water film
V	= freestream air velocity
We_d	= Weber number based on droplet diameter, $\rho_w V^2 d / \sigma$
We_t	= Weber number based on water film thickness, $\rho V^2 t_w / \sigma$
β	= local collection efficiency
ΔC_p	= change in pressure coefficient in the nose region of the body

θ	= position angle in nose region of body
μ, μ_w	= viscosity of air, viscosity of liquid water
ρ, ρ_w	= density of air, density of liquid water
σ	= surface tension of liquid water
τ	= icing test run time
τ_0	= aerodynamic shear stress exerted on the surface of the water film

Subscripts

Mod, Ref	= model and reference cases, respectively
0	= stagnation point, except for τ_0
∞	= freestream conditions

Introduction

THE large amounts of refrigeration needed for icing wind tunnels place severe restraints on their size. The possibility of conducting valid icing tests at reduced scale is thus particularly attractive. Unfortunately, scaling laws for icing testing are not yet fully established. The objective of this paper is to review knowledge gained as a result of the substantial efforts devoted to this issue in recent years.

In-flight icing occurs when supercooled liquid water droplets in clouds impinge onto the leading edges of aircraft surfaces. The impinging droplets tend to freeze, releasing the latent heat of fusion, and this tends to increase the temperature of the surface. In rime icing, convective and evaporative heat loss to the ambient air is sufficient to keep the surface temperature below the freezing point, and all of the impinging droplets freeze completely immediately upon impact. In glaze icing, on the other hand, the rate of convective/evaporative heat loss is less than the rate at which heat of fusion would be released if the droplets were to freeze completely upon impact. Consequently, only a certain fraction, the freezing fraction, of the impinging water freezes upon impact, and the remainder runs back to freeze elsewhere. Glaze icing tends to occur when liquid water content (LWC) of the clouds is relatively high and the ambient air temperature is only a little below the freezing point, 0°C. The behavior of the runback water has a very important influence on the ice accretion process.

The relatively simple scaling requirements for rime icing will first be briefly considered. The remainder of the paper will focus on the scaling requirements for glaze icing conditions. The term *reference* will be used to denote the flight and icing conditions that are to be simulated, and *model* will denote the test conditions used for the simulation. Parameters are said to be matched if they have equal values in the model and reference cases.

Received 18 November 2002; presented as Paper 2003-1216 at the 41st Aerospace Sciences Meeting, Reno, NV, 6–9 January 2003; revision received 24 March 2003; accepted for publication 31 March 2003. Copyright © 2003 by R. J. Kind. Published by the American Institute of Aeronautics and Astronautics, Inc., with permission. Copies of this paper may be made for personal or internal use, on condition that the copier pay the \$10.00 per-copy fee to the Copyright Clearance Center, Inc., 222 Rosewood Drive, Danvers, MA 01923; include the code 0001-1452/03 \$10.00 in correspondence with the CCC.

*Professor, Department of Mechanical and Aerospace Engineering, Associate Fellow AIAA.

Scaling of Rime Icing

It is becoming increasingly recognized that rime icing can be reliably scaled,¹ using scaling procedures developed by French researchers more than two decades ago.² Figure 1 shows examples of successful scaling of rime ice accretion shapes. As just mentioned, in rime icing the impinging droplets freeze completely where they impact onto the surface. Therefore, successful scaling only requires flowfield and droplet-trajectory similarity and correct scaling of the amount of supercooled water accumulated on the body during test runs. These requirements are readily satisfied by using geometrically scaled models, matching the nondimensional droplet-trajectory and accumulation parameters K and Ac , respectively, and using a sufficiently low freestream air temperature so that the freezing fraction n is 1.0 everywhere on the ice surface. K and Ac are defined in the Appendix, which also outlines the procedure for determining test conditions.

Scaling of Glaze Icing: An Overview

Current computer codes are capable of giving good and reliable predictions of rime icing so the main experimental interest is in glaze icing where icing computer codes still have serious shortcomings.³ Moreover, glaze ice accretion shapes tend to be more complex and more detrimental to aerodynamic performance than rime ice accretion shapes. Contrary to the situation with rime icing, complete scaling laws for glaze icing are not yet established, although considerable progress has been made over the previous decade or so, as outlined in the remainder of this paper.

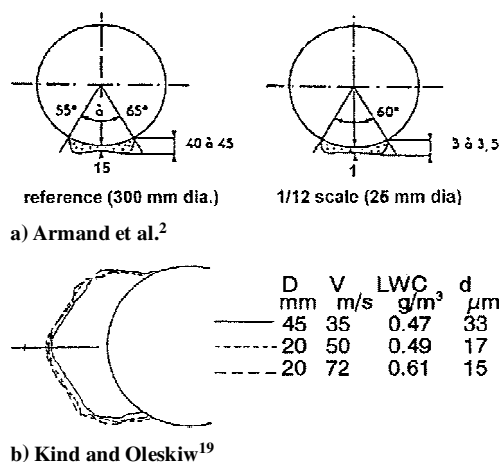


Fig. 1 Examples of scaling of rime icing.

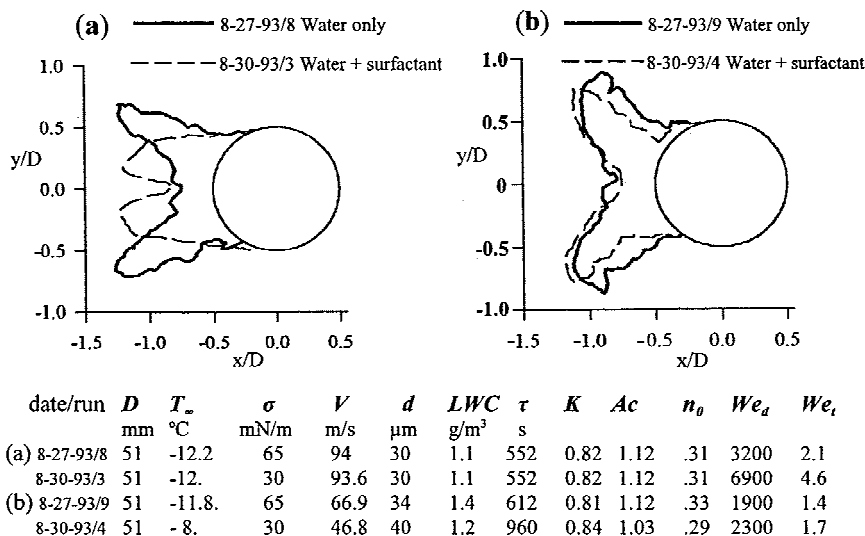


Fig. 2 Examples of effects of changing surface tension and of Weber-number scaling with constant cylinder diameter (results of Bilanin and Anderson^{10,11}).

Much testing, notably by Anderson,⁴⁻⁸ has been done in the effort to identify scaling requirements for glaze icing. In general only modest size-reduction ratios, about 3:1 or less, have been attempted, and icing test conditions have mainly been within the FAR 25-Appendix C envelope. Since the early work of Armand et al.² and Ruff,⁹ there has been recognition that flowfield and droplet-trajectory similarity are necessary and that the accumulation parameter and the freezing fraction n_0 at the stagnation point should have the same values in model and reference cases. Testing to date has supported these requirements, but in some of the tests scaling success was good whereas in others it was poor. This indicates that the aforementioned requirements are necessary, but not sufficient, to ensure scaling success. In other words, the experimental evidence suggests that current practices for scaling of glaze icing tests do not recognize one or more important parameters.

In glaze icing, liquid water is present on the surface of the ice accretion in the droplet-impingement region. This water tends to run back, driven by aerodynamic forces. The behavior of this run-back water is very important in determining the ice accretion shape for two reasons: first, it determines where the water moves to and eventually freezes; and second, surface tension effects tend to cause formation of beads and rivulets, which, before or after freezing, can act as surface roughness that can strongly influence the convective heat loss to the ambient air. Recognizing this, Bilanin and Anderson¹⁰ pointed out that surface tension of the water is probably important. Indeed they demonstrated that addition of surfactants to the spray water in an icing test "had a dramatic effect on the shape of the ice." The importance of surface tension is illustrated by Fig. 2a,^{10,11} which shows ice-shape tracings for two test runs in which all parameters except surface tension had the same values. The ratio of aerodynamic forces to surface-tension forces is known as the Weber number. Bilanin and Anderson¹⁰ proposed that a Weber number We_d , based on spray-droplet diameter, be added to the list of similarity requirements for glaze icing tests. Figure 2b^{10,11} exemplifies the good scaling success they achieved when this Weber number was approximately matched for the model and reference cases in their tests on circular cylinders. Anderson¹² reported further encouraging results a year later. However, as testing continued, it became apparent that although scaling success was usually quite good when Weber number based on droplet diameter was matched it was sometimes significantly better in other cases,¹³ suggesting that there were still some unresolved scaling issues.

Note that for the two runs of Fig. 2b, in addition to the Weber number, the other similarity parameters mentioned earlier K , Ac , and n_0 are also matched (approximately). As outlined in the Appendix, the required matching can be achieved by choosing mean droplet diameter d to match K , LWC, to match n_0 , run time τ to match Ac , and freestream velocity V to match the Weber number. The Weber

number is, in effect, the velocity scaling parameter. The freestream air temperature $T_{\infty \text{Mod}}$ in the model test appears at this point to be a free parameter that can be chosen arbitrarily. Obviously, however, it is necessary to match the distribution of freezing fraction n over the entire ice accretion surface, not just its stagnation-point value n_0 . As will be seen later, this imposes constraints on the choice of $T_{\infty \text{Mod}}$. Another issue is choosing the most appropriate length scale for the Weber number.

Length Scale in Weber Number

When surface tension effects are important in aerodynamically driven liquid flows, the ratio of aerodynamic forces to surface-tension forces is a relevant similarity or scaling parameter. This ratio, easily shown to be $\rho V^2 \ell / \sigma$, is known as the Weber number. Note that ρ should be the density of the air, not of the liquid, because $\rho V^2 \ell^2$ is a measure of the aerodynamic forces, whereas $\sigma \ell$ is a measure of the surface-tension forces.

The length scale ℓ in the Weber number must be appropriate to the physical process whose scaling is being considered. There is currently some disagreement regarding a suitable choice for ℓ . Possible candidates are the overall body size L , the supercooled droplet mean diameter d , or some measure of the thickness of the water flow on the ice-accretion surface. Because the requirement is to scale the surface water flow dynamics correctly, the appropriate length scale would seem to be a measure of the thickness of this flow. Because this thickness is very small, the body size L should be of little direct relevance. Also the droplet diameter d should be of little direct relevance to this flow because the droplets disappear as distinct entities upon impact; d would, however, be relevant to splashing if this occurs upon droplet impact.

The liquid water that is present on the surface of glaze ice accretions initially forms a thin film in the stagnation region. Although this film breaks up into beads and rivulets a short distance downstream, it would seem that assuming a spanwise-uniform film and calculating its thickness would yield an average liquid water thickness that would be suitable for scaling purposes. Because the film is very thin, it is reasonable to assume laminar equilibrium flow, with negligible inertia effects.^{14,15} This means that the flow in the water film can be considered as a superposition of two-dimensional Couette and Poiseuille flow because it is driven by the shear stresses and pressure gradients imposed on it by the airflow. Using a relation for water-mass conservation and a superposition of the classical Couette and Poiseuille flow solutions, Kind¹⁶ derived expressions for the water film thickness t_w and for the mean velocity u_w in the water film. The expression for t_w is

$$t_w^2 = \frac{\mu_w L W C V \beta (1 - n) (D/2) \sin \theta}{\rho_w (0.5 \rho V^2) (C_f/2 + 0.42 \Delta C_p t_w / D)} \quad (1)$$

For working purposes the values of β , D , θ , C_f , and ΔC_p were set to 1.0, chord times thickness ratio, 45 deg, 0.003, and -2 , respectively, for evaluation of Eq. (1). Scaling results are insensitive to these estimated values because we are primarily concerned with ratios for model to reference cases; β , θ , C_f , ΔC_p , and also n should have the same values for the model and reference cases so that they largely cancel out of the ratios. Kind¹⁶ proposed that t_w , as given by Eq. (1), be used as the length scale in the Weber number, that is, that matching of $\rho V^2 t_w / \sigma$ be used for velocity scaling in glaze icing tests.

Values of t_w calculated from Eq. (1) for typical glaze icing conditions are, as expected, very small, of order 10^{-5} m. This suggests that the ratio of viscous forces to surface-tension forces in the water flow is also important. This ratio is given by the capillary number $\mu_w u_w / \sigma$. It is interesting that the expression for $\mu_w u_w / \sigma$ is identical to that for the Weber number $\rho V^2 t_w / \sigma$ when the analysis outlined here is used to determine u_w and t_w . Upon reflection, this is not surprising because the analysis for the water film thickness t_w assumes that the aerodynamic and viscous forces are in equilibrium. Thus, matching of $\rho V^2 t_w / \sigma$ automatically ensures matching of $\mu_w u_w / \sigma$, which is fortunate.

If splashing is important when the supercooled droplets impact onto the liquid film on a glaze ice accretion, a Weber number that uses droplet diameter as the length scale, that is, $\rho_w V^2 d / \sigma$, would be important in addition to $\rho V^2 t_w / \sigma$. The former is the Weber number proposed by Bilanin and Anderson.¹⁰ On the basis of Walzel's¹⁷ correlation, Kind¹⁶ argues that splashing probably is important in typical glaze icing conditions. Moreover, recent high-speed video imagery acquired at the NASA Icing Research Tunnel contains evidence that splashing does indeed occur under some conditions.¹⁸ As seen later, both of the Weber numbers mentioned in this paragraph can be approximately matched simultaneously under certain conditions.

Assessment of Water-Film-Thickness Weber Number

Reference 16 includes an assessment of the proposed new scaling parameter $We_t = \rho V^2 t_w / \sigma$. The approach taken was to use results of scaling tests reported in the literature and examine whether there was any correlation between good scaling success and approximate matching of $\rho V^2 t_w / \sigma$ in corresponding model and reference cases. Only results for cases where K , Ac , and n_0 were matched (within 10, 5, and 15%, respectively) were considered. Runs with freestream Mach number above 0.4 were excluded to rule out possible compressibility effects. Figures 3 and 4 present results for test runs where scaling success was judged to be "good" and "weak," respectively. It can be said that there is some correlation between good scaling success and approximate matching of We_t (Fig. 3) and vice versa (Fig. 4). There was no deliberate attempt made to match We_t in any of the test runs of Figs. 3 and 4. As seen in Fig. 5, correlation between good scaling success and approximate matching of $We_d = \rho_w V^2 d / \sigma$ was somewhat less good than that seen in Fig. 3, except for test runs where We_d was deliberately matched. Approximate matching of We_d was deliberate for all of the points within about $\pm 5\%$ of the perfect-match line in Fig. 5. Because the droplets lose their identity upon impact, droplet diameter d and the Weber number We_d can be expected to be of little direct relevance to the water flow on the ice surface and thus to icing scaling, unless splashing occurs upon droplet impact. To the extent that there is some correlation between good scaling and matching of We_d , as seen in Fig. 5, this might be because matching of $We_d = \rho_w V^2 d / \sigma$ results in approximate matching of $We_t = \rho V^2 t_w / \sigma$ and vice versa, as seen later. Figure 6, also from Ref. 16, presents a plot of model vs reference values of t_w / c , the ratio of water film thickness to overall body size. There is clearly a tendency for the relative thickness of the water film to be greater in the subscale test runs when the usual scaling methods are used. This implies that there will be some

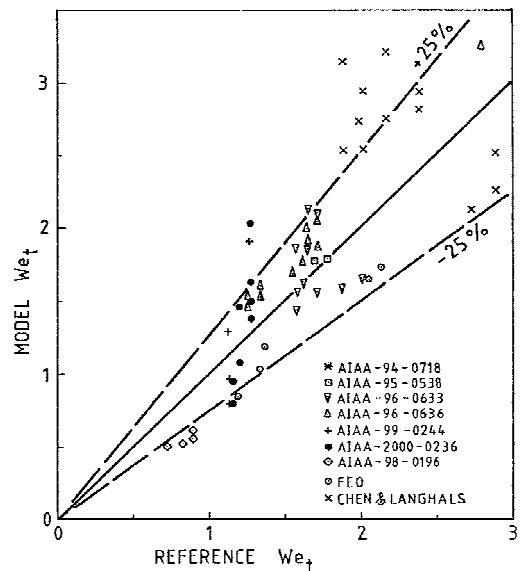


Fig. 3 Correlation of good scaling success with matching of We_t (from Kind¹⁶).

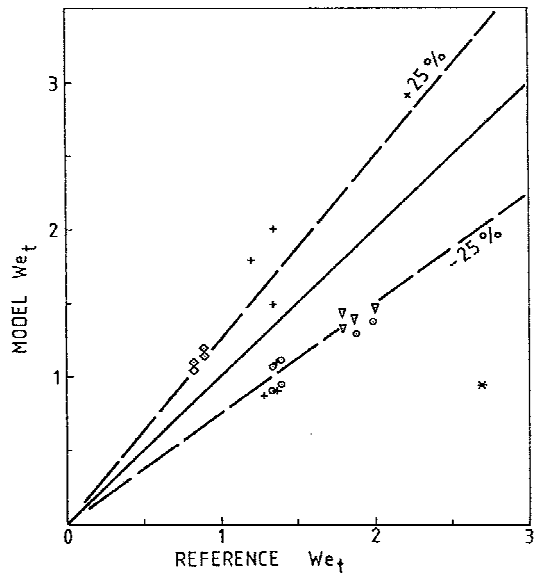


Fig. 4 Correlation of weak scaling success with matching of We_t (from Kind¹⁶; legend as in Fig. 3).

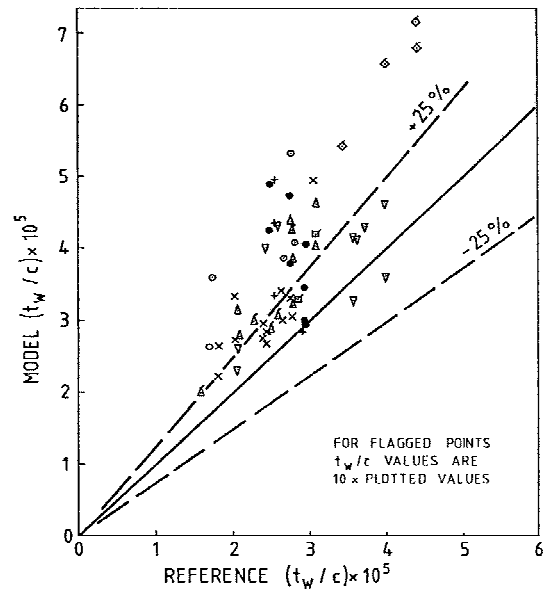


Fig. 6 Model vs reference t_w/c for test runs with good scaling success (from Kind¹⁶; legend as in Fig. 3).

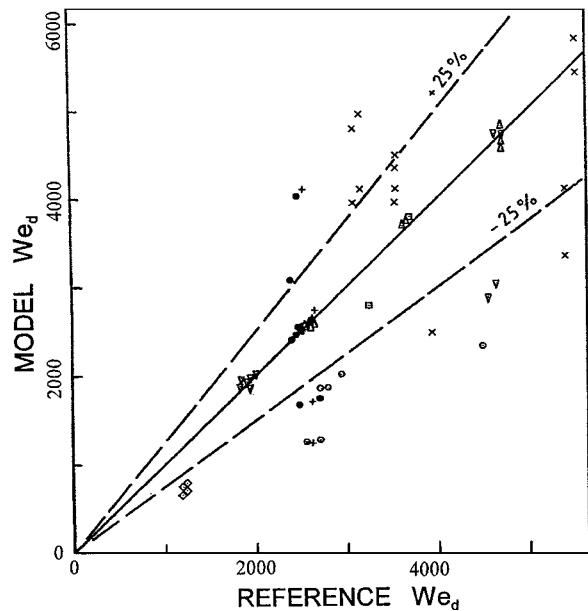


Fig. 5 Correlation of good scaling success with matching of We_d (from Kind¹⁶; legend as in Fig. 3).

difference in test conditions determined using the Weber number based on water film thickness We_t for scaling as compared with using a Weber number based on body size as the length scale. As discussed earlier, the water film thickness is considered to be the more appropriate length scale.

To convey a more concrete sense of the situation, a few sets of ice shape tracings from recent papers are presented in Figs. 7–10. In each of these figures K , Ac , and n_0 have approximately the same values, whereas velocity V , and thus We_t , change from one subscale run to the next. In Fig. 7 scaling success is quite good for the $We_t = 0.9$, 1.1, and 1.5 subscale runs, consistent with the value of 1.35 in the reference case. As pointed out by one of the referees, the total and recovery temperatures in the $We_t = 2.0$ subscale run of Fig. 7 are very near 0°C , and this is probably a more important factor than the mismatch in We_t for the poor scaling success in this run. Because the ice surface is at 0°C , the temperature difference driving the convective heat transfer in this test run is very small, and minor local variations in this difference would have a disproportionate effect on the distribution of local freezing fraction. More

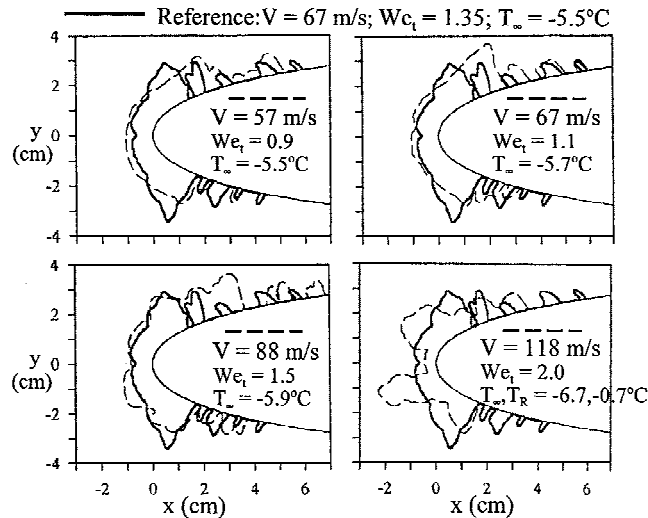


Fig. 7 Examples of scaling results for various freestream velocity values; results of Anderson and Ruff.¹³ (NACA-0012 airfoil at $\alpha = 0$; reference chord = 53.3 cm; subscale chord = 27.7 cm; subscale ice coordinates doubled; K , Ac , $n_0 = 0.10, 0.05, 0.3$ for all cases).

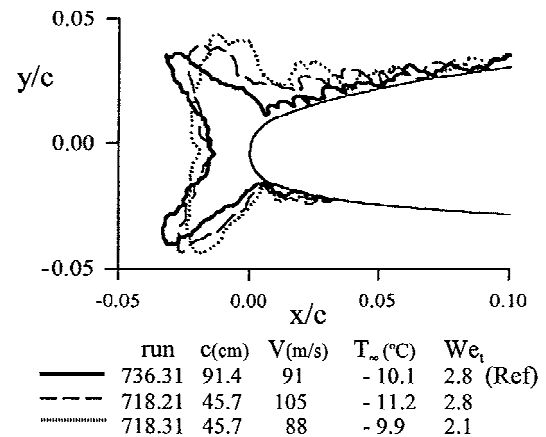


Fig. 8 Additional examples of scaling results (from Anderson¹¹): GLC-305 airfoil at $\alpha = 0$; K , Ac , $n_0 = 0.085, 0.06, 0.3$ for all cases.

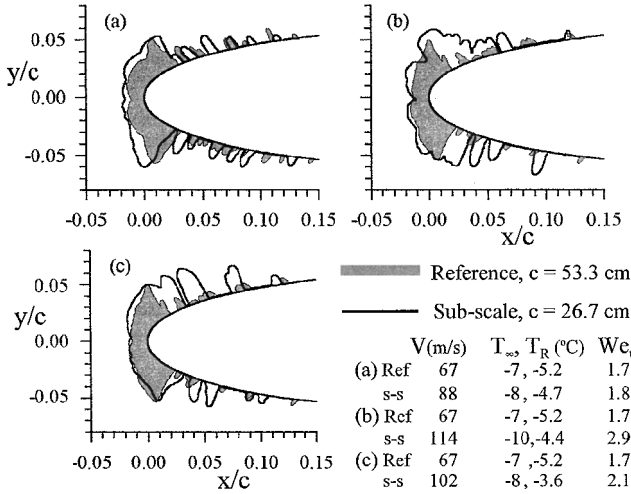


Fig. 9 Examples of repeatability and scaling (from Anderson⁸): NACA-0012 airfoil at $\alpha = 0$; $K, A_c, n_0 \approx 0.10, 0.055, 0.28$ for all cases.

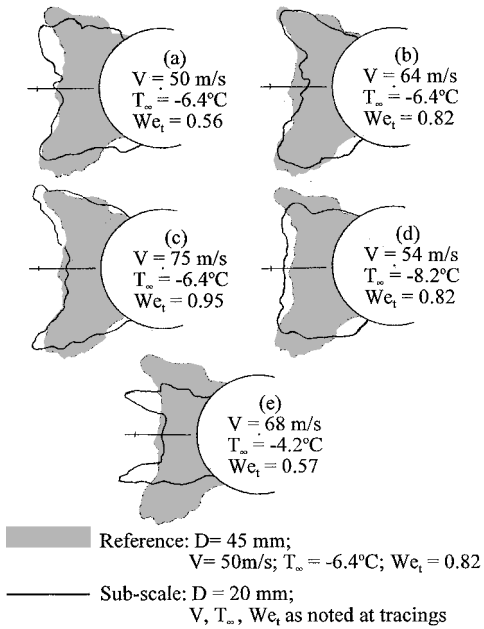


Fig. 10 Examples of scaling tests for circular cylinders, showing effects of varying velocity and temperature; results of Kind and Oleskiw¹⁹; $K, A_c, n_0 = 0.32, 1.1, 0.3$ for all cases.

discussion of this will be presented later. In Fig. 8 $We_t = 2.8$ for the reference case, and the ice shape for the subscale run with $We_t = 2.8$ is a somewhat better match to the reference shape than that for the run with $We_t = 2.1$.

In Fig. 9 the reference ice shape tracings are from three distinct test runs for nominally the same test conditions. Comparison reveals substantial variation between the three repeat tracings. This is typical and must always be borne in mind when comparing glaze ice shape tracings. The velocity and We_t have various values in the three subscale runs of Fig. 9. Given the variability between repeat runs, a definite assessment of which velocity value gives the best scaling success is not possible, although scaling success appears best in Fig. 9a, where $We_{t,Mod} \approx We_{t,Ref} = 1.7$. In Figs. 7 and 9 the weakest scaling success occurs when the Mach number is relatively high ($M \geq 0.35$). This seems to be a frequent occurrence at least when the freezing fraction is relatively low, say, below 0.3. Compressibility effects, mismatch of We_t values, and total temperature substantially above the reference values could be contributing factors to the poor scaling in such cases. The last factor would appear to be relatively unimportant in the case of Fig. 9, however, where

the total temperature in the subscale run of Fig. 9b, at -3.7°C , is only 1.3°C above the reference value. In Fig. 10 scaling success is best in Fig. 10b and 10c for which the values of We_t are close to the reference value of 0.82 and ambient air temperature T_∞ is equal to the reference value. Figure 10 illustrates an observation that applies to all of the results of Ref. 19, namely, that scaling success was quite good for the entire range of velocities, $0.85 < V/V_{Ref} < 1.5$ provided that T_∞ was essentially equal to the reference value; however, even if the temperature in a subscale test run differed by only a few degrees from the reference value there was a distinct deterioration in scaling success, as seen for example in Figs. 10d and 10e.

Observations from the Assessment Work

A number of observations were made in the course of the assessment work outlined in the preceding section. They include the following:

1) Within a range of about $0.85 < V/V_{Ref} < 1.5$, scaling success appeared to be insensitive to the criterion used to determine wind speed, but was perhaps marginally better when the Weber number based on water-film thickness, $We_t = \rho V^2 t_w / \sigma$, was used for this purpose. As might be expected, the quality of scaling appears to be more sensitive to wind speed at lower values of the stagnation-point freezing fraction n_0 , presumably because more of the impinging water remains liquid and thus mobile after impingement.

2) Although freestream air temperature has been considered to be a free parameter up to this point, when it differed from the value used in the reference case, scaling success deteriorated markedly in some tests.

3) When freestream air temperature was chosen equal to that in the reference case and the Weber number based on water-film thickness was matched, the Weber number $We_d = \rho_w V^2 d / \sigma$, based on spray droplet diameter, was also approximately matched.

Figure 11 illustrates observation 3. It presents a plot of the ratio We_d / We_t for a large number of subscale and reference run pairs for which T_∞ and We_t were approximately matched. Points that fall close to the line of perfect agreement in Fig. 11 indicate that We_d was also approximately matched for that run pair. It would be very fortunate if observation 3 were generally valid because the requirements for dynamic similarity of splashing behavior, mentioned earlier, would then be approximately satisfied. Note that $We_d = \rho_w V^2 d / \sigma$ cannot in practice be varied independently because d must be chosen to match the droplet trajectory parameter K .

Observations 2 and 3 will be discussed in the following section.

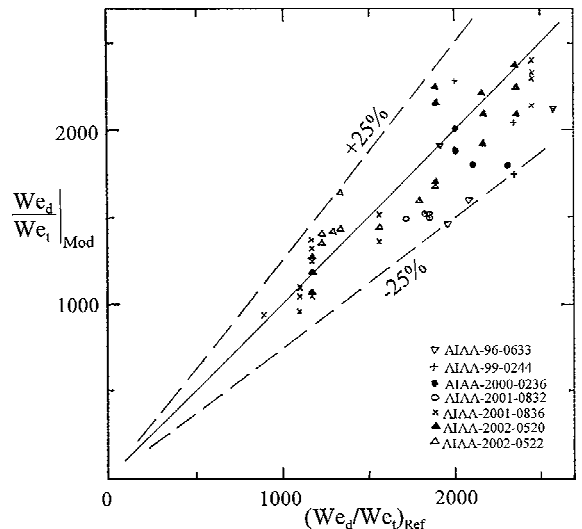


Fig. 11 Correlation plot of ratio We_d / We_t for model and reference scaling run pairs for which K, A, n_0 , and We_t match within 10, 10, 15, and 20%, respectively.

Discussion

Kind²⁰ recently suggested the following explanation for observation 2 of the preceding section. Using the Messenger²¹ model, the expression for the freezing fraction can be shown to consist of the sum of two nondimensional terms, that is,²²

$$n = \frac{(A + B/\beta)}{(1 + m_r/m_i)}$$

where

$$A = \frac{C_w(T_i - T_\infty - V^2/2C_w)}{h_{fs}}$$

$$B = \frac{(1 + q_c/q_c)h_c(T_i - T_R)}{(LWCVh_{fs})} \quad (2)$$

The runback mass flow rate m_r can be disregarded in this discussion. Note that A has a constant value, whereas B varies with position in the ice-accretion region because the convective heat-transfer coefficient h_c of course varies. Thus, the B term in Eq. (2) represents a distribution, with a particular value B_0 at the stagnation point. If we require that $n_{0Mod} = n_{0Ref}$ and choose $(T_\infty + V^2/2C_w)_{Mod} = (T_\infty + V^2/2C_w)_{Ref}$, then $A_{Mod} = A_{Ref}$ and $B_{0Mod} = B_{0Ref}$, and it is reasonable to expect that the B term in Eq. (2) will make the same contribution to the distribution of n as in the reference case. On the other hand, if $(T_\infty + V^2/2C_w)_{Mod} \neq (T_\infty + V^2/2C_w)_{Ref}$, then $A_{Mod} \neq A_{Ref}$ and $B_{0Mod} \neq B_{0Ref}$; n_{Mod} will then equal n_{Ref} only at the stagnation point, and the distributions of B and n will differ from the reference case. This explanation is supported by computations carried out using the icing codes TRAJICE2 (Gent, R. W., private communication, DERA, United Kingdom, Feb. 2001) and LEWICE2 (McDowall, R., private communication, May 2001), results of which are shown in Figs. 12 and 13. It would thus appear that the values of the sensible/latent and convective/latent heat ratios, A and B , should be individually matched at the stagnation point. In practice, the freezing droplets are water in both the reference and the reduced scale cases so matching of n_0 and of T_∞ is equivalent to matching of A and B_0 , provided that the kinetic energy terms $V^2/2C_w$ and $V^2/2C_p$ have approximately the same values in the model and reference cases. Despite the preceding, scaling results are not always sensitive to mismatches of freestream temperature. For example, unlike the results in Figs. 10d and 10e, in scaling tests on NACA-0012 airfoils Oleskiw et al.²³ did not observe any distinct deterioration in scaling success when the freestream temperature was varied by up to 3°C. Also in Fig. 2b there is a significant temperature difference, yet scaling is good. Nevertheless the preceding argument indicates that it would be prudent to limit mismatch of freestream temperature or of the sensible/latent heat ratio A insofar as possible.

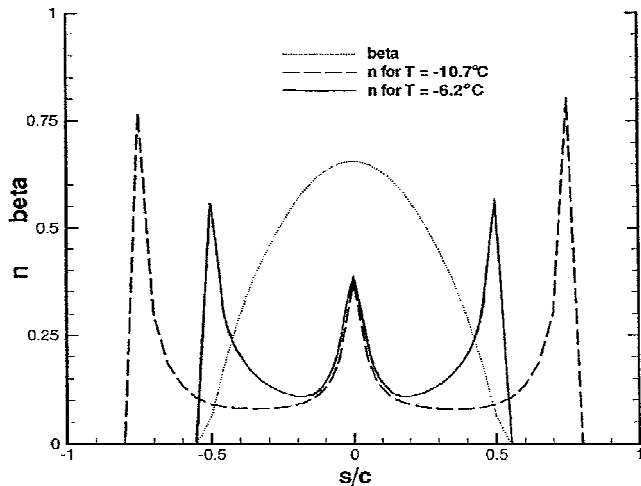


Fig. 12 Collection efficiency and freezing fraction distribution predicted by TRAJICE2 (Gent, private communication) for 20-mm-diam cylinders with same K , Ac , n_0 , and We_t but different T_∞ .

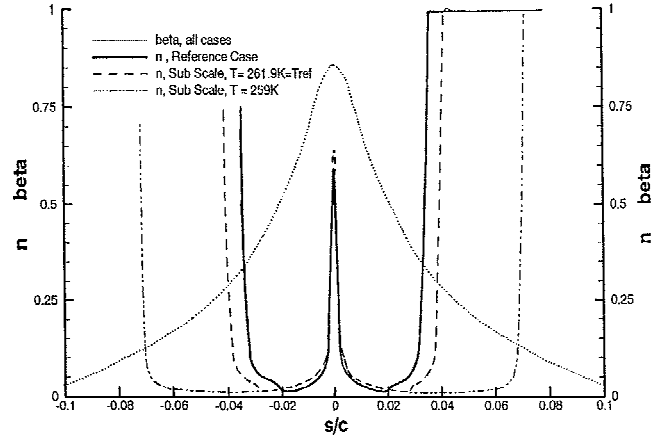


Fig. 13 Collection efficiency and freezing fraction distribution predicted by LEWICE2 (McDowall, private communication) for NACA-0012 airfoils at $\alpha = 0$ with same K , Ac , n_0 , and We_t but different T_∞ : $c = 500$ mm for reference and 222 mm for subscale cases.

When considering Fig. 7, it was noted that a major factor in the poor scaling success in the test run with $V = 118$ m/s, $We_t = 2.0$ might well be that the total and recovery temperatures in this run were 0 and -0.7°C , respectively. This can be understood if one recognizes that the assumption that convective heat-transfer rate is proportional to $h_c(T_i - T_R)$, used in the expression for B in Eq. (2), is a simplification which might well break down when $(T_i - T_R)$ approaches zero. For example, the local heat sink temperature might well vary somewhat from the recovery temperature T_R as the flow proceeds around the ice accretion, especially if the Mach number is relatively high, and this would have a relatively large effect on the distributions of convective heat-transfer rate and freezing fraction when $(T_i - T_R)$ approaches zero. It would be prudent to avoid using subscale test velocities that result in excessive $(T_{RMod} - T_{RRef})/(T_i - T_{RRef})$ values; it is far from clear what the upper limit for this ratio should be, but 0.3 is an interim suggestion. The ratio has a value of 0.8 for the aforementioned test run of Fig. 7.

An analysis has been carried to assess if observation 3 of the preceding section is purely coincidental or not. We assume that the spray water and air properties and all of the parameters in Eq. (1), except LWC , V , D , and t_w , have the same values in the model and reference cases. If water film thickness t_w is determined from Eq. (1) and the droplet diameter d and LWC are determined from the relations in the Appendix such that K and B_0 are matched, then using these relations it can be shown that

$$\frac{(d/t_w)_{Mod}}{(d/t_w)_{Ref}} = \frac{(V_{Mod}L_{Mod})^{0.2}}{(V_{Ref}L_{Ref})^{0.2}} \quad (3)$$

Recall that L is the body size which is an overall length scale of the airflow. Equation (3) holds, regardless of what criterion is used to establish velocity scaling. If V_{Mod}/V_{Ref} is chosen such that the Weber number We_t , based on water-film thickness is matched, then we obtain

$$\frac{(d/t_w)_{Mod}}{(d/t_w)_{Ref}} = \frac{(V_{Ref})^{0.08}(L_{Mod})^{0.12}}{(V_{Mod})^{0.08}(L_{Ref})^{0.12}} \quad (4)$$

Because of the small exponent values, the ratio in Eq. (4) has a value of approximately unity. Because d/t_w is proportional to the ratio of Weber numbers We_d/We_t , this implies that $(We_d/We_t)_{Mod} \approx (We_d/We_t)_{Ref}$, which explains observation 3) and shows that it is not merely coincidental. This is very fortunate because it implies that splashing, if it occurs, will be scaled approximately correctly if the procedures outlined herein are used to determine test conditions.

In some glaze icing situations large beads of liquid water can accumulate in regions where aerodynamic forces are quite high. Liquid water may then be “stripped” by the airflow, that is to say, is removed from the ice accretion. The scaling considerations outlined herein should cover this situation if it arises.

Conclusions

Successful physical modeling of rime icing is possible at reduced scale and requires only that Reynolds-number effects be small, that the droplet trajectory and accumulation parameters K and Ac be matched to their reference values, and that T_∞ is low enough to ensure that the freezing fraction is 1.0 everywhere.

The work of the past decade has extended and clarified scaling requirements for glaze icing, and indications are that all of the apparent scaling requirements can be met at least approximately for size-scale ratios less than about 3:1 and icing conditions within the FAR 25-Appendix C envelope.

In glaze icing the flow behavior of the liquid water on the surface of the ice accretion is very important both by virtue of its strong influence on the convective heat-transfer rate and by virtue of determining where the runback water moves to and eventually freezes. Both surface tension and water viscosity have significant effects on this behavior. Scaling requirements should take this into account. A Weber number We_t , based on water-film thickness, has been proposed for this purpose, and preliminary assessment suggests that it might have merit.

In both full-scale and reduced-scale glaze icing tests the distribution of freezing fraction should match that in the reference case. This requires matching of both the sensible/latent and convective/latent heat ratios A and B at the stagnation point. In practice, this is usually equivalent to matching the static temperature of the freestream air and the stagnation-point freezing fraction n_0 .

Scaling success appears to usually be only mildly sensitive to freestream velocity and temperature, and so Weber-number scaling and matching of the sensible/latent heat ratio A can often be considerably relaxed. However, caution is advised when doing so. Caution is also advised when the recovery temperature approaches 0°C .

It has been shown that if the nondimensional parameters K , A , B , and We_t are matched to their reference values, then the Weber number We_d relevant to splashing is also approximately matched. All of the tentatively known requirements for scaling of glaze icing would then be matched.

It would appear that satisfactory results are obtainable from reduced-scale glaze icing tests. Much further testing is required to substantiate this and to hopefully extend it to supercooled large droplet and three-dimensional conditions. It is recommended that, where feasible, future icing wind-tunnel test programs include some amount of reduced-scale testing in order to expand the experience base. Further work is also needed to isolate the effects of high Mach number, total temperature near 0°C , and high Weber-number ratios.

Appendix: Relations Used to Determine Conditions for Reduced-Scale Icing Test Runs

Values of c , V , p_∞ , T_∞ , LWC , MVD , and run or exposure time τ are assumed to be known for the reference cases. Values of c and p_∞ can be chosen as convenient for the subscale model test runs. The surface tension σ and other water properties are assumed to have the same values in the reference and model cases. Using the relations listed next, MVD , τ , and LWC for the subscale runs are chosen such that K , Ac , and n_0 are equal to the reference values. Freestream velocity V is chosen to satisfy an appropriate criterion, for example, to match $We_t = \rho V^2 t_w / \sigma$ to the reference value, as proposed in this paper, with t_w given by Eq. (1). The ambient air temperature T_∞ is chosen to match A to the reference value. The air stagnation temperature T_0 is evaluated from the adiabatic relation. An estimate of 1.0 can be used for β_0 if no better estimate is available; in any case droplet-trajectory scaling ensures that β is matched for model and reference cases so that ratios are insensitive to it. The formulas for h_c and q_e/q_c were derived from relations given in Ref. 24:

$$Ac = \frac{LWC V \tau}{(c \rho_w)}$$

$$K = \left(\frac{1}{18}\right) \left(\frac{\rho_w}{\rho}\right) \left(\frac{d}{c}\right) \left(\frac{\rho V d}{\mu}\right)^{0.65}$$

where MVD is used for d (Ref. 25):

$$n_0 = A + B_0/\beta_0$$

at the stagnation point, where there is no runback water entering the control volume,²²

$$A = \frac{C_w (T_i - T_\infty - V^2/2C_p)}{h_{fs}}$$

$$B = \frac{(1 + q_e/q_c) h_c (T_i - T_R)}{(LWC V h_{fs})}$$

where T_R is given by

$$T_R = T_\infty + Pr^{0.333} (V^2/2C_p)$$

h_c is given by

$$h_c = [0.0239(k/L)(\rho V L/\mu)^{0.80}]$$

and q_e/q_c is given by

$$q_e/q_c = \frac{1518(p_{\text{vap},273} - p_{\text{vap},T_\infty})}{(273 - T_R)} = \frac{0.64(273 - T_\infty)}{(273 - T_R)}$$

k , C_p , and Pr are the thermal conductivity, specific heat at constant pressure, and Prandtl number of the air. The preceding formula for h_c gives the average value for a smooth circular cylinder, and it is used to get a rough estimate of h_c . The actual local h_c will vary strongly around ice accretions, but values are unknown. For scaling purposes the value of the exponent is most important as the other factors cancel out of the ratios; we use 0.8 because test results reported in Ref. 23 gave this value at the stagnation line.

Acknowledgment

The author is grateful for financial support from the Natural Sciences and Engineering Research Council of Canada through its Research Grants program.

References

- Kind, R. J., and Oleskiw, M. M., "Recent Developments in Scaling Methods for Icing Wind Tunnel Testing at Reduced Scale," International Congress of the Aeronautical Sciences, Paper 2002-7.3.1, Sept. 2002.
- Armand, C., Charpin, F., Fasso, G., and Leclerc, G., "Techniques and Facilities at the ONERA Modane Centre for Icing Tests," AGARD Advisory Report No. 127, Appendix to Paper 6, Nov. 1978.
- Kind, R. J. (ed.), *Ice Accretion Simulation Evaluation Test*, NATO/RTO, TR-038, Nov. 2001.
- Anderson, D. N., "Rime-, Mixed- and Glaze-Ice Evaluations of Three Scaling Laws," AIAA Paper 94-0718, Jan. 1994.
- Anderson, D. N., "Methods for Scaling Icing Test Conditions," AIAA Paper 95-0540, Jan. 1995.
- Anderson, D. N., "Effect of Velocity in Icing Scaling Tests," AIAA Paper 2000-0236, Jan. 2000.
- Anderson, D. N., "A Preliminary Study of Ice-Accretion Scaling for SLD Conditions," AIAA Paper 2002-0521, Jan. 2002.
- Anderson, D. N., "Ice-Accretion Scaling Using Water-Film Thickness Parameters," AIAA Paper 2002-0522, Jan. 2002.
- Ruff, G. A., "Analysis and Verification of the Icing Scaling Equations," Arnold Engineering Development Center, AEDC-TR-85-30, Arnold Air Force Station, TN, March 1986.
- Bilanin, A. J., and Anderson, D. N., "Ice Accretion with Varying Surface Tension," AIAA Paper 95-0538, Jan. 1995.
- Anderson, D. N., "Acceptable Tolerances for Matching Icing Similarity Parameters in Scaling Applications," AIAA Paper 2001-0832, Jan. 2001.
- Anderson, D. N., "Evaluation of Constant-Weber-Number Scaling for Icing Tests," AIAA Paper 96-0636, Jan. 1996.
- Anderson, D. N., and Ruff, G. A., "Evaluation of Methods to Select Scale Velocities in Icing Scaling Tests," AIAA Paper 99-0244, Jan. 1999.
- Towell, G. D., and Rothfeld, L. B., "Hydrodynamics of Rivulet Flow," *AICHE Journal*, Vol. 12, Sept. 1966, pp. 972-980.
- Myers, T. G., and Thompson, C. P., "Modeling the Flow of Water on Aircraft in Icing Conditions," *AIAA Journal*, Vol. 36, No. 6, 1998, pp. 1010-1013.
- Kind, R. J., "Assessment of Importance of Water-Film Parameters for Scaling of Glaze Icing," AIAA Paper 2001-0835, Jan. 2001.

¹⁷Walzel, P., "Zerteilgrenze beim Tropfenprall," *Chemie Ingenieur Technik*, Vol. 52, No. 4, 1980, pp. 348, 349 (in German).

¹⁸Bond, T., informal presentation, Society of Automotive Engineers, AC-9C meeting, April 2002.

¹⁹Kind, R. J., and Oleskiw, M. M., "Experimental Assessment of a Water-Film-Thickness Weber Number for Scaling of Glaze Icing," AIAA Paper 2001-0836, Jan. 2001.

²⁰Kind, R. J., "Some Issues in Physical and Computational Modelling of Glaze Icing," *Proceedings of the 48th Annual Conference of the Canadian Aeronautics and Space Institute (CASI)*, Vol. 1, edited by V. Nguyen, Canadian Aeronautics and Space Inst., Ottawa, 2001, pp. 595–604.

²¹Messinger, B. L., "Equilibrium Temperature of an Unheated Icing Surface as a Function of Air Speed," *Journal of the Aeronautical Sciences*, Vol. 20, 1953, pp. 29–42.

²²Kind, R. J., Potapczuk, M. G., Feo, A., Golia, C., and

Shah, A. D., "Experimental and Computational Simulation of In-Flight Icing Phenomena," *Progress in Aerospace Sciences*, Vol. 34, 1998, pp. 257–345.

²³Oleskiw, M. M., McCullough, T., and Kind, R. J., "Further Assessment of a Proposed Additional Scaling Parameter and of Non-Matching Freestream Temperature for Glaze Icing Tests," AIAA Paper 2002-0520, Jan. 2002.

²⁴Kreith, F., *Principles of Heat Transfer*, 2nd ed., International Textbook Co., Scranton, PA, 1965, Chaps. 9, 13.

²⁵Bragg, M. B., "A Similarity Analysis of the Droplet Trajectory Equation," *AIAA Journal*, Vol. 20, 1982, pp. 1681–1686.

J. P. Gore
Associate Editor